Contents lists available at ScienceDirect

Corrosion Science

Electrochemical corrosion studies of spark plasma sintered zirconia particle-reinforced high-alloy steel at different temperatures

Marcel Mandel [*], Lutz Krüger, Sabine Decker

Technische Universität Bergakademie Freiberg, Institute of Materials Engineering, Gustav-Zeuner-Straße 5, 09599 Freiberg, Germany

A B S T R A C T

The influence of temperature on the corrosion behaviour of spark plasma sintered high-alloy steel – with particle reinforcement using 10 vol.% partially stabilised zirconia – was investigated. The cyclic polarisation behaviour and electrochemical impedance were analysed in a 5 wt.% sodium chloride solution. It was found that the corrosion potential was not influenced by temperature. However, the anodic polarisation behaviour and impedance exhibited significant declines in polarisation resistance when the temperature increased. A homogeneous corrosion attack was observed at 25 °C and 35 °C, while an intensified particle detachment and subsequent pitting corrosion occurred at 45 °C and 55 °C.

© 2014 Elsevier Ltd. All rights reserved.

1. Introduction

Metal matrix composites (MMCs) offer many advantages for engineering, such as increased strength, wear resistance, and hardness. By Tian et al. [1] an increase of the yield stress and elongation was found for the aluminium alloy 2024 by addition of ZrB_2 nanoparticles. The observed improvement in mechanical behaviour was attributed to a grain-refinement effect of the alloy matrix induced by the particles. Martin et al. [2] investigated a zirconia particle reinforced steel. They attached the strengthening effect to a phase transformation in the steel matrix and in the particles. Furthermore, Li [3] showed enhanced mechanical qualities in tensile strength and hardness of the TiB_2 reinforced zinc–aluminium ZA27 matrix alloy composite. It was pointed out, that the increased strength correlates to a homogeneous particle distribution, a strong matrix/particle interfacial bonding and an interaction between dislocations and the particles. A similar behaviour of a SiC particle reinforced aluminium based composite was presented by Vijayavel et al. [4]. In the studies of Lü et al. [5] and Krüger et al. [6], the improvement of the mechanical properties in dependence of increasing particle content was demonstrated. In addition, the enhancing effect in hardness and wear resistant of a TiC particulates locally reinforced manganese steel matrix was shown by Hu et al. [7]. In summary, the observed improved mechanical characteristics

are commonly provided by the combination of a ductile metal matrix with rigid particles. However, compared to their unreinforced counterparts, the corrosion resistance of particle-reinforced materials is often reduced. It has been observed that, particle reinforcement increases corrosion sensitivity, and that corrosion is initiated at the interface between the particle and the metal matrix [8–13]. Therefore, electrochemical behaviour is dictated by particle size and particle content. In a corrosive environment, the electrochemical behaviour depends on the corrosion kinetics at the surface. Austenitic stainless steels are a good alternative for providing acceptable corrosion stability and, ultimately, good component durability [14]. However, the presence of chlorides influences the integrity of the surface, and thus the occurrence of pitting corrosion. A characteristic parameter for evaluating pitting susceptibility is the critical pitting temperature (CPT), which defines a potential-independent temperature, below which pitting corrosion is not observed [15–20]. Furthermore, the influence of temperature is used to analyse the polarisation characteristics and electrochemical impedance behaviour [20,21] to obtain information about the reaction kinetics at the material/electrolyte interface [22,23]. Electrochemical impedance spectroscopy (EIS) is a well-established method for analysing the structure and properties of solid/electrolyte interfaces [24]. Several models have been developed to describe the impedance behaviour of an electrode using a combination of simple elements such as resistors, capacitors, or inductors. To consider surface effects like porosity or roughness, the capacity is commonly expressed by a constant phase element (CPE), with the impedance Z_{CPE} defined by Eq. (1):

* Corresponding author. Tel.: +49 3731393176; fax: +49 3731393703.
  E-mail address: mandel@iwt.tu-freiberg.de (M. Mandel).

$$Z_{CPE} = \frac{1}{Q(j\omega)^{\alpha}},\qquad(1)$$

where Q is the CPE parameter, α the CPE exponent, $j = (-1)^{1/2}$ the imaginary unit, and ω the angular frequency [25–27]. Two methods in particular have been employed, to obtain information about the effective capacity of an electrode. Brug et al. propose a model that considers the local inhomogeneities along an interface, which are described by a surface time-constant distribution [28]. In addition, Hsu and Mansfeld describe the impedance of an electrode by means of a normal time-constant distribution, which involves the addition of each component perpendicular to the surface [29]. Both theories are widely used to derive the effective capacity from CPE parameters. The Brug formulas are applied for studies on hydrogen and oxygen evolution processes [30,31] or passive films [32], whereas the Hsu and Mansfeld formulas are used for studies on protective coatings [33,34]. When considering the time-dependent electrochemical degradation of an electrode, the Brug formulas can be assumed to explain the corrosion behaviour of the initial state before the corrosion, while the Hsu and Mansfeld formulas can be employed to explain the corrosion behaviour after the corrosion, when a surface film has formed. In Fig. 1, schematic illustrations of the corresponding equivalent circuits for surface and normal distributions are shown, as presented by Hirschorn et al. [26].

In both theories, local electrode components were combined to form global elements to determine the effective capacity. The relation between the CPE parameters Q and α and the effective capacity C_{eff} developed by Brug et al. is given in Eq. (2). For a normal distribution, the relation defined by Hsu and Mansfeld is given by Eq. (3).

$$C_{eff} = \left[Q \left(\frac{1}{R_e} + \frac{1}{R_t} \right)^{\alpha-1} \right]^{\frac{1}{\alpha}}\qquad(2)$$

$$C_{eff} = Q^{1/\alpha} R_f^{(1-\alpha)/\alpha}\qquad(3)$$

R_e is the ohmic resistance of the electrolyte, R_t is the global interface resistance, and R_f is the film resistance. Finally, the corresponding

time constants τ_{eff} for both surface and normal distribution are given by Eqs. (4) and (5), respectively.

$$\tau_{eff} = \frac{R_e R_t}{R_e + R_t} C_{eff}\qquad(4)$$

$$\tau_{eff} = R_f C_{eff}\qquad(5)$$

If the time constant is known, information about the interface reaction kinetic can be determined. Joiret et al. [35] and Rodriquez-Lopez et al. [36] observe multiple time constants on iron and magnetite electrodes. In both studies, the time constant at high frequencies is correlated to charge-transfer processes in the double layer, whereas at intermediate frequencies, the time constant is attributed to redox processes. In consideration of an electrochemical degradation, the reaction kinetics are controlled by charge-transfer processes under the initial state, whereas after degradation, redox processes in the layer generated by a film formation are added.

To date, the mechanical behaviour of particle-reinforced materials has been well investigated, whereas less is known about the electrochemical behaviour of particle-reinforced high alloy steel. In particular, the influence of temperature is mostly discussed for unreinforced materials. In the present study, the influence of temperature on the electrochemical corrosion behaviour of a new developed MgO partially stabilised zirconia (Mg-PSZ) particle-reinforced high-alloy steel, was investigated using low scan-rate cyclic voltammetry, electrochemical impedance spectroscopy and potentiostatic polarisation.

2. Experimental

High-alloy steel powder, with its main alloying elements of 14 wt.% Cr, 6 wt.% Mn, and 6 wt.% Ni, was milled with 10 vol.% MgO partially stabilised zirconia (Mg-PSZ) powder. The chemical compositions of the steel powder and the Mg-PSZ powder are presented in Tables 1 and 2.

The particle size of the Mg-PSZ powder was determined by laser diffraction using a particle analyser (Beckman-Coulter, LS230). The powder mixture was sintered in a spark plasma sintering device (FCT-HP 25, diameter of die = 20 mm) by heating at 100 K/min up to a temperature of 1100 °C. The load was increased to 51 MPa in parallel to the increasing temperature, and kept constant through the dwell time of 5 min. Afterwards, the specimens were allowed to cool to room temperature in an unregulated manner. The samples density was determined by Archimedes' method. For electrochemical investigation, machined round test specimens with an area of 0.5 mm^2 were prepared and embedded in epoxy resin to avoid crevice corrosion by the sealing ring (opening cross section 0.785 mm^2) of the electrochemical test station. Afterwards, the sintered specimens were ground with SiC and polished with a diamond suspension to 1 μm. To observe the microstructure, the polished samples were etched with the Beraha II solution (parent solution: 800 cm^3 distilled water, 400 cm^3 HCl, and 48 g (NH$_4$)HF$_2$; for etching: 100 cm^3 parent solution +1 g K$_2$S$_2$O$_5$). The grain size of the steel matrix was microscopically evaluated by the linear intercept method applying five line scans and the particle to matrix ratio was determined by the binarisation method. For the line intercept and binarisation method the a4i Analysis V5.10a software was used.
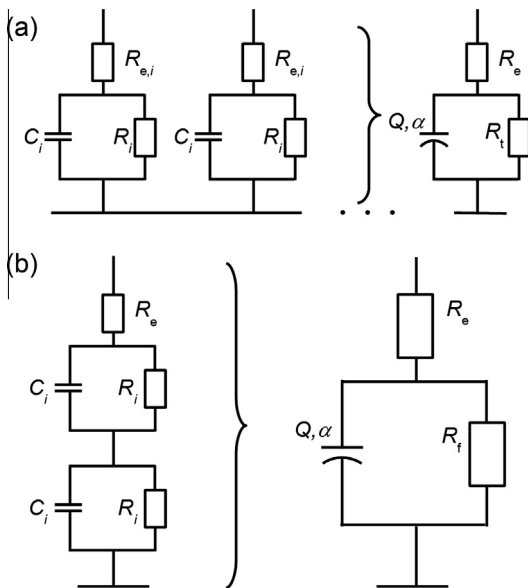

Fig. 1. Illustration of equivalent circuits for impedance behaviour of the metal/film/electrolyte interface: (a) in the case of surface distribution, and (b) in the case of normal distribution [19]. $R_{e,i}$, R_i, C_i, denote the local electrolyte resistance, charge transfer resistance, and local capacity, respectively; R_e, R_t, R_f denote the global electrolyte resistance, charge transfer resistance, and film resistance, respectively; Q and α are the global CPE parameters.

Table 1
Chemical composition of the high-alloy steel powder in wt.%.

Cr	Mn	Ni	Si	Al	N (ppm)	C	S	Fe
14.02	6.14	6.11	0.91	0.11	388.00	0.04	0.02	Balance